

**GENTAMICIN-LOADED POLY (LACTIC ACID)
MICROSPHERE CORPORATED CHITOSAN-
COATED CARBONATE APATITE SCAFFOLD**

**NORMAHIRA BINTI MAMAT @ MOHAMAD
NOR**

UNIVERSITI SAINS MALAYSIA

2019

**GENTAMICIN-LOADED POLY (LACTIC ACID)
MICROSPHERE CORPORATED CHITOSAN-
COATED CARBONATE APATITE SCAFFOLD**

by

**NORMAHIRA BINTI MAMAT @ MOHAMAD
NOR**

**Thesis submitted in fulfilment of the requirements
for the degree of
Doctor of Philosophy**

May 2019

ACKNOWLEDGEMENT

Alhamdulillah, all praises to ALLAH the almighty. Most grateful gratitude belongs to HIM for conferring me health and endurance in completing this thesis. HE has granted the countless bounties to enable me accomplishing such challenging yet interesting experience in my life. There were also many people who have contributed along my research endeavours.

First and foremost, my utmost appreciation goes to my supervisor, Professor Ir Dr Mariatti Jaafar. I would not have achieved what I have been able if not for her expertise, guidance, enthusiasm and persistent help in achieving my research goals and Ph.D. I will forever be indebted to her encouragement, support and advice. I would also like to thank my co-supervisor Dr Zuratul Ain Abdul Hamid for her willingness to assist me and give comments throughout this journey.

My deepest thanks also go to Associate Prof Dr Badrul Hisham Yahaya who allowed me to use the facilities for doing cell culture in Regenerative Medicine Center (RMC) at Advanced Medicine and Dentistry Institute (AMDI), Universiti Sains Malaysia (USM). His invaluable advices are unforgettable. Special thanks are extended to Dr Nurazreena and Dr Khairul Anuar Shariff for their opinions and invaluable suggestions in completing my research.

My sincere thanks go to the dean, staff and assistant engineers in School of Materials and Mineral Resources Engineering (SMMRE), USM who had contributed in my study. My genuine gratitude is also deserved to my lab mates including Fadilah, Rosaniza, Shuyen, Iqbal, Meer and Nurulain. It was a pleasure working with them and I really appreciate their help. I would also like to thank all postgraduate students in SMMRE, USM for their knowledge sharing.

Next, I am deeply thankful to my employer, Universiti Malaysia Perlis (UniMAP) who gave me the opportunity to continue my study and Ministry of Education Malaysia for the financial support throughout my study period.

My warmest appreciation goes to my family and family-in-law. Thank you for your constant love and support as I pursued my Ph.D. Any thanks and appreciation to my loving mother would not be enough. She has constantly inspired me and do prayers in whatever I have been through in my life. I am also blessed to have my beloved husband. His unconditional love, devotion, and encouragement helped me to endure the demands of this journey. Finally, to my daughter, Nuha Nafeesa, she is the one young spirit who makes me more motivated to finish this journey. Thank you all for your endless love, support and understanding.

TABLE OF CONTENT

ACKNOWLEDGEMENT	ii
TABLE OF CONTENT	iv
LIST OF TABLES	x
LIST OF FIGURES	xii
LIST OF SYMBOLS	xix
LIST OF ABBREVIATIONS	xx
ABSTRAK	xxii
ABSTRACT	xxiv
CHAPTER 1 INTRODUCTION	1
1.1 Background of study	1
1.2 Problem Statement	4
1.3 Objectives.....	6
1.4 Scopes of research.....	7
1.5 Thesis Organization	8
CHAPTER 2 LITERATURE REVIEW	10
2.1 Introduction	10
2.2 Characteristic of human bone.....	10
2.2.1 Composition and structure of bone	10
2.2.2 Mechanical properties of bone	12
2.2.3 Bone remodeling	13
2.3 Concern and current materials used in scaffolds.....	14
2.4 Bone tissue engineering	17
2.4.1 Scaffolds requirements	18
2.4.2 Fabrication of porous scaffold.....	20

2.5	Bioceramics for bone scaffold	20
2.5.1	Hydroxyapatite (HA).....	22
2.5.2	Tricalcium phosphate (TCP)	25
2.5.3	Ionic-substituted apatite	26
2.5.3(a)	Carbonate substitutes apatite	27
2.5.3(b)	Transformation of TCP to CO ₃ Ap.....	29
2.6	Polymers coating on bone scaffold	32
2.6.1	Chitosan (CS)-coated bone scaffolds	34
2.6.2	Surface treatment and polymer coating	36
2.7	Localized bone healing by drug-loaded bone scaffold	40
2.7.1	Fabrication and modification of drug loaded microsphere.....	43
2.7.2	Drug loaded scaffold for bone healing process	47
2.7.2(a)	<i>In vitro</i> , mechanical performance and bioactivity	51
2.7.2(b)	Drug release kinetics	52
2.8	Biological performance of bone scaffold.....	54
2.8.1	<i>In vitro</i> evaluation in simulated body fluid/ Hanks' balanced salt solution.....	55
2.8.2	<i>In vitro</i> evaluation using cell culture	57
2.9	Interaction between host cell and biomaterials	57
2.10	Summary	59
CHAPTER 3 MATERIALS AND METHODOLOGY		60
3.1	Introduction	60
3.2	Raw Materials	61
3.3	Experimental procedures.....	65
3.3.1	Fabrication of β -TCP scaffold.....	65
3.3.1(a)	Preparation of β -TCP slurry	65
3.3.1(b)	Freezing, freeze drying and sintering	66

3.3.2	Transformation of porous β -TCP scaffold to carbonate apatite (CO ₃ Ap) scaffold	68
3.3.3	Silane treatment on CS-coated CO ₃ Ap scaffold.....	69
3.3.3(a)	Preparation of silane solution, GA solution and CS solution	69
3.3.3(b)	Chitosan-coated CO ₃ Ap scaffold without surface treatment	70
3.3.3(c)	Chitosan-coated CO ₃ Ap scaffold with surface treatment	70
3.3.4	Surface modification of gentamicin (GEN)-loaded PLA microsphere	72
3.3.4(a)	Preparation of PLA microsphere and GEN-loaded PLA microsphere	72
3.3.4(b)	Surface Modification of PLA microsphere	73
3.3.4(c)	Percentage of encapsulation efficiency and drug loading of neat GENMS and modified GENMS	74
3.3.4(d)	Protein adsorption on neat GENMS and modified GENMS using bovine serum albumin (BSA).	75
3.3.5	Fabrication of uncoated and coated CO ₃ Ap scaffold incorporated by GEN	76
3.3.5(a)	Preparation of CO ₃ Ap scaffold incorporated by GEN solution	77
3.3.5(b)	Coating process on CO ₃ Ap scaffold with GEN and GENMS in CS solution	77
3.4	Characterization techniques	78
3.4.1	X-ray Diffraction (XRD).....	78
3.4.2	Fourier-transform infrared spectroscopy (FTIR).....	79
3.4.3	Scanning Electron Microscopy (SEM) and energy dispersive X-ray (EDX).....	80
3.4.4	Elemental Analyzer (CHN)	80
3.4.5	Porosity measurement	81
3.4.6	Compressive strength	81
3.4.7	Viscosity test	82

3.4.8	Water absorption	82
3.4.9	Ultraviolet-Visible (UV-Vis) spectrophotometer.....	83
3.4.10	Drug release assessment.....	83
3.4.10(a)	Kinetic mechanism of drug release	83
3.4.10(b)	Antibacterial assessment.....	85
3.4.11	Particle size.....	86
3.4.12	Zeta potential	87
3.4.13	Contact angle	87
3.4.14	<i>In vitro</i> bioactivity evaluation of CO ₃ Ap scaffold: Immersion in Hank's Balance Salt Solution (HBSS).....	88
3.4.15	Inductively Coupled Plasma (ICP) Spectroscopy	90
3.4.16	Degradation rate	90
3.4.17	<i>In vitro</i> evaluation on the biocompatibility of scaffold: Cell study	91
3.4.17(a)	Sample preparation	91
3.4.17(b)	Cell culture using Human osteoblast-like cells (hFOB)..	91
3.4.17(c)	Cell detachment and cell counting prior to seeding on the sample.....	91
3.4.17(d)	Cell proliferation.....	93
3.5	Statistical analysis	93
CHAPTER 4 RESULTS AND DISCUSSION.....		94
4.1	Introduction	94
4.2	Porous CO ₃ Ap scaffold fabricated by hydrothermal treatment	94
4.2.1	Effect of different molar on carbonate content and Ca/P ratio.....	94
4.2.2	XRD and FTIR analysis of CO ₃ Ap scaffold	96
4.2.3	Microstructures of CO ₃ Ap scaffold.....	101
4.2.4	Evaluation of porosity and compressive strength.....	103
4.2.5	<i>In vitro</i> bioactivity evaluation	105

4.2.5(a)	Biodegradation.....	105
4.2.5(b)	Ca/P ratio, surface charge and apatite formation.....	106
4.2.6	Cell proliferation	110
4.3	Surface modification of CO ₃ Ap scaffold with silane solution and coating with chitosan	112
4.3.1	Compressive strength, porosity and morphology of CS-coated CO ₃ Ap scaffold	112
4.3.2	FTIR analysis and EDX of silanised CO ₃ Ap scaffold	117
4.3.3	Swelling ratio	120
4.3.4	<i>In vitro</i> bioactivity	122
4.3.4(a)	Biodegradation.....	122
4.3.4(b)	Morphology and EDX analysis	125
4.3.5	Relation between surface charge and cell proliferation	130
4.4	Effect of surface modification on GEN-loaded PLA microsphere using alkaline hydrolysis	133
4.4.1	Determination of microsphere size.....	133
4.4.2	Encapsulation efficiency and drug loading of GEN-loaded PLA microsphere	137
4.4.3	FTIR and morphology of GEN-loaded PLA microsphere after surface modification.....	138
4.4.4	Surface wettability, surface energy and zeta potential	141
4.4.5	Protein adsorption by BSA.....	143
4.4.6	Encapsulation efficiency and drug loading of modified GENMS and GEN release profile	146
4.5	Fabrication of CO ₃ Ap scaffold incorporated with GEN-loaded PLA microsphere	150
4.5.1	XRD phase analysis.....	151
4.5.2	FTIR and morphology of CO ₃ Ap scaffold incorporated with GEN	152
4.5.3	Porosity and compressive strength	156
4.5.4	Swelling ratio	158

4.5.5	Drug release profile and kinetics mechanism.....	159
4.5.6	<i>In vitro</i> bioactivity	165
4.5.6(a)	Biodegradation.....	165
4.5.6(b)	Apatite formation.....	167
4.5.6(c)	EDX analysis	171
4.5.7	Antibacterial inhibition zone assessment by gram positive and gram negative bacteria	173
4.5.8	Cell proliferation	176
CHAPTER 5	CONCLUSIONS AND RECOMMENDATION.....	178
5.1	Conclusions	178
5.2	Recommendation for Future Work	179
REFERENCES.....		181
APPENDIX A: CALCULATION FOR PREPARING SILANE SOLUTION		
APPENDIX B: CALCULATION OF ENCAPSULATION EFFICIENCY (%) AND DRUG LOADING (%)		
APPENDIX C: KINETIC PLOTS OF GENTAMICIN RELEASE FROM SAMPLES		
LIST OF PUBLICATIONS		

LIST OF TABLES

	Page
Table 2.1 Chemical composition of bone (wt%) (Eliaz and Metoki, 2017)	12
Table 2.2 Mechanical properties of corticol and trabecular bone (Ramay and Zhang, 2004; Murugan and Ramakrishna, 2005).....	13
Table 2.3 Fabrication methods developed 3D porous bone scaffolds incorporated with therapeutic drug-delivery capability	20
Table 2.4 Chemical composition of CaP (Laskus and Kolmas, 2017)	22
Table 2.5 Ions substitution and function in CaP	26
Table 2.6 Comparison between A- and B-type CO ₃ Ap (Landi <i>et al.</i> , 2004; LeGeros <i>et al.</i> , 1969).....	28
Table 2.7 Parameters affecting carbonate content of CO ₃ Ap	32
Table 2.8 Recent studies on polymer-coated scaffolds for BTE.....	34
Table 2.9 Types of silane coupling agent used for HA modification	38
Table 2.10 Utilization of silane for coating of bone substrate and improved mechanical properties (%).....	40
Table 2.11 Selected experimental trials carried out for 3D bone scaffolds with a combination of broad spectrum antibiotics	42
Table 2.12 Different approaches for the delivery of antibiotics using bioceramic scaffolds.....	48
Table 3.1 Ionic compositions and concentration (mmol.dm ⁻³) of biological fluids and media formulations (Rabadjieva <i>et al.</i> , 2009; Ye <i>et al.</i> , 2014)	64
Table 3.2 Raw materials used in experimental method	64
Table 3.3 Composition and designation of coated-CO ₃ Ap scaffolds used in the study	71
Table 3.4 Formulation of PLA and PVA used in this study	72

Table 3.5	Designation and composition of GEN incorporated CO ₃ Ap scaffold.....	78
Table 3.6	Classification of the release mechanism depending on sample geometry and the release exponent n of the Peppas model (Hess <i>et al.</i> , 2017)	84
Table 3.7	Operating conditions of instrument and spectral line of analytes	90
Table 4.1	Quantitative data of Ca, P and CO ₃ – content (wt.%) and the molar Ca/P ratio using 3 and 5M Na ₂ CO ₃ solutions for 3, 5 and 7 D of hydrothermal treatment.....	95
Table 4.2	Crystallographic properties of produced CO ₃ Ap scaffolds. Peak positions (2 θ /degree) at maximum intensity and FWHM (2 θ /degree) of the (0 0 2) peaks. HA properties is used as reference (Ebrahimi <i>et al.</i> , 2017)	98
Table 4.3	Crystallite size and crystallinity of fabricated CO ₃ Ap scaffolds	99
Table 4.4	EDX results of molar Ca/P ratio of 5D3M and 5D5M scaffolds for 3, 7, 14, and 28 days immersion in HBSS	106
Table 4.5	The molar Ca/P ratio of UTR and TR scaffolds after 7 and 28 days immersion in HBSS solution.....	128
Table 4.6	The concentration variations of PVA used for making microspheres of 18% total mixtures of PLA-PVA	134
Table 4.7	Contact angle and surface energy of modified GENMS.....	142
Table 4.8	Zeta potential of neat GENMS and modified GENMS in HBSS solution.....	143
Table 4.9	EE and DL of neat GENMS and modified GENMS.....	147
Table 4.10	Release kinetic parameters calculated from the GEN release data in PBS solution using different mathematical models describing drug release mechanisms (R ² =correlation coefficient; n=diffusional release exponent representing the type of transport) .	163
Table 4.11	Mechanism of drug release from system	165

LIST OF FIGURES

	Page
Figure 2.1 The multiscale of natural bone and its composition (Gao <i>et al.</i> , 2017)	11
Figure 2.2 Bone remodeling begins with osteoclasts followed by osteoblast and osteocytes (Kapinas and Delany, 2011)	14
Figure 2.3 A schematic of the evolution of bioceramics (reproduced from Wang <i>et al.</i> , 2012).....	16
Figure 2.4 Three basic element in TE concept (Swaminathan and Thomas, 2013)	17
Figure 2.5 Crystal structure of the HA (Wijesinghe, 2014)	23
Figure 2.6 SEM image of osteoclasts on the surface of (a) the bone and (b) sintered HA (Antoniac, 2016).....	24
Figure 2.7 SEM image of CO ₃ Ap after 12 weeks <i>in vivo</i> . (a) Grain boundary dissolution in the crystallites. (b) At several triple-junctions, an entire grain had dissolved away (Porter et al., 2005).....	29
Figure 2.8 Typical force-displacement curves of non-coated and coated bioglass scaffold under compressive loading (Philippart <i>et al.</i> , 2015)	33
Figure 2.9 Chemical structure of chitosan (CS) (Rodríguez-Vázquez, 2015)...	35
Figure 2.10 Organofunctional silane molecule basic structure and schematic of silanization on an oxide ceramic surfaces (Treccani <i>et al.</i> , 2013)	39
Figure 2.11 Schematic overview of four principal process steps in microsphere preparation by ESE (Freitas <i>et al.</i> , 2005).....	44
Figure 2.12 Chemical structure of PLA.....	45
Figure 2.13 The hydrolysis of ester bond in PLA backbone chains created carboxyl and hydroxyl end group	46

Figure 2.14	Release of profile of (a) gentamicin, (b) TTC and (c) daidzen from free microspheres, uncoated scaffolds and microsphere-coated scaffolds (Francis <i>et al.</i> , 2010; Macías-Andrés <i>et al.</i> , 2017; Meng <i>et al.</i> , 2013)	50
Figure 2.15	Mechanism of drug release from particulate system (Unagolla and Jayasuriya, 2018).....	53
Figure 2.16	SEM images of apatite formed (a) (left) on surface and (right) cross section of glass-ceramic A–W, (b) on surface of treated titanium and (c) on surface of silica gel (Kokubo and Takadama, 2006)	55
Figure 3.1	Overview flowchart for the whole experimental work	61
Figure 3.2	Chemical structure of 3-(Trimethoxysilyl) propyl methacrylate	62
Figure 3.3	Schematic diagram on fabrication of S- β -TCP using gelate-freeze casting method	66
Figure 3.4	Heat treatment regime for the fabrication of S- β -TCP scaffold.....	67
Figure 3.5	Flowchart for fabrication β -TCP scaffold	67
Figure 3.6	Flowchart for fabrication and characterization porous CO ₃ Ap scaffold.....	69
Figure 3.7	Schematic diagram for fabrication and characterization of untreated (TR) (route I) and treated (UTR)(route II) CO ₃ Ap scaffold.....	71
Figure 3.8	Schematic of double ESE process to produce GEN-loaded PLA microspheres	73
Figure 3.9	Standard curve of GEN from absorbance intensity at 195 nm and GEN concentration from 10 – 400 ppm.....	74
Figure 3.10	Schematic diagram of BSA adsorption measurement by neat GENMS and modified GENMS	75
Figure 3.11	Standard curve of BSA from absorbance intensity at 279 nm and BSA concentration between 100- 1500 ppm	76
Figure 3.12	Schematic diagram of GEN-loaded CO ₃ Ap scaffold.....	77

Figure 3.13	Schematic of agar diffusion test for antimicrobial testing	86
Figure 3.14	A submerged specimen in HBSS solution in falcon tube	89
Figure 3.15	Flowchart for <i>in vitro</i> bioactivity test	89
Figure 3.16	Counting area using hemocytometer by 4 squares.....	92
Figure 4.1	XRD patterns of CO ₃ Ap scaffold for 3, 5 and 7 D of treatment in (a) 3M (b) 5M Na ₂ CO ₃ solution. XRD pattern of standard HA is shown as a reference	97
Figure 4.2	FTIR spectra of fabricated CO ₃ Ap scaffolds for 3, 5 and 7 D in (a) 3M and (b) 5M Na ₂ CO ₃	100
Figure 4.3	SEM images and aspect ratio values of S-β-TCP scaffold (a) before and (b-g) after hydrothermal treatment: 3M (left side) and 5M (right side) Na ₂ CO ₃ for 3D (b and c), 5D (d and e) and 7D (f and g). (Images of a, b, c, d, e, f and g were observed at 200× magnification, images of insert were observed at 2500× magnification, values of aspect ratio for respective images are based on 30 measurements)	102
Figure 4.4	Compressive strength and porosity of S-β-TCP, 5D3M and 5D5M CO ₃ Ap scaffolds. * indicates $p < 0.05$ compared between groups ..	104
Figure 4.5	<i>In vitro</i> biodegradation of CO ₃ Ap scaffolds for 3, 7, 14, 21 and 28 d in HBSS solution.....	105
Figure 4.6	(a) Zeta potentials of CO ₃ Ap surface at pH 7. (b) pH measurement of HBSS solution after 3, 7, 14, 21, and 28 days immersion. * indicates $p < 0.05$ compared between groups	107
Figure 4.7	SEM morphologies show apatite growth of (a) (i,ii) 5D3M and (b) (i,ii) 5D5M scaffolds after 28 days immersion in HBSS. EDX spectra show mineral deposition on (a) 5D3M and (b) 5D5M after (iii) 3 days and (iv) 28 days immersion. (Images of (a and b) (i) and (a and b) (ii) were observed at 1000× and 7000× magnification, respectively)	109

Figure 4.8	Proliferation of hFOB cells for CO ₃ Ap scaffolds measured by PrestoBlue after days 1, 2, 3, 5 and 7 at 37 °C.....	111
Figure 4.9	Compressive strength and percentage porosity of neat, UTR and TR CO ₃ Ap scaffolds. * indicates a significant difference ($p < 0.05$) at the same coating concentration	113
Figure 4.10	SEM images of pore structure (left) and coating layers (right) on CO ₃ Ap scaffolds. (a and b) neat CO ₃ Ap, coated CO ₃ Ap scaffolds of (c and d) 0.5% CS, (e and f) 1% CS and (g and h) 2% CS. (Images of a, c, e and g were observed at 60× magnification, images of b, d, f and h were observed at 5000× magnification)	115
Figure 4.11	Schematic illustration of steps used to chemically bond CS to the neat CO ₃ Ap scaffold via silane treatment	117
Figure 4.12	(A) FTIR spectra of (a) neat CO ₃ Ap, (b) silanised-CO ₃ Ap, (c) pure CS, (d) UTR0.5, (e) TR0.5, (f) UTR2 and (g) TR2. (B) The enlargement of FTIR spectra from 1000 to 1800 cm ⁻¹	118
Figure 4.13	SEM images and EDX spectra shows elemental composition of (a) neat CO ₃ Ap and (b) silanised-CO ₃ Ap scaffolds (Images were observed at 15000× magnification).....	120
Figure 4.14	Swelling behaviour of the CO ₃ Ap scaffolds in PBS solution. Dotted line shows UTR scaffolds and solid line shows TR scaffolds	121
Figure 4.15	Interaction of CS layer on (a) with silanisation and (b) without silanisation of CO ₃ Ap scaffold showed by red circle. (Images were observed at 15000× magnification).....	122
Figure 4.16	<i>In vitro</i> biodegradation for 3, 7, 21 and 28 days in 37 °C HBSS solution of CO ₃ Ap scaffolds	123
Figure 4.17	Concentration of Ca in HBSS solution for 3, 7, 14, 21, and 28 days immersion of CO ₃ Ap scaffolds. Dotted line shows UTR scaffolds, solid line shows TR scaffolds	124
Figure 4.18	SEM images of (a) UTR0.5, (b) TR0.5, (c) UTR1, (d) TR1, (e) UTR2 and (f) TR2. Images (i) and (ii) are before and after 28 days	

	immersion in HBSS, respectively (Images were observed at 7000× magnification)	126
Figure 4.19	Schematic diagram on the mechanism of apatite formation on the TR scaffold in HBSS.....	129
Figure 4.20	Zeta potential of different surface CO ₃ Ap scaffolds at pH 7.0 of HBSS. * indicates p < 0.05 is significantly difference	130
Figure 4.21	The results of PrestoBlue assay for silanised-, UTR0.5 and TR0.5 CO ₃ Ap scaffolds in the presence of hFOB cells for 7 days incubation.....	132
Figure 4.22	SEM images of PLA microsphere size, (a) PLA 15% and (b) 9%. (Images (i) and (ii) observed at 1000 × and 3000 ×, respectively) ..	135
Figure 4.23	Distribution size of fabricated PLA microsphere. (a) 15%, (b) 10% and (c) 9%	136
Figure 4.24	Size of GENMS fabricated through double ESE technique. (Images were observed at 1500× (left) and 3000× (right)).....	137
Figure 4.25	FTIR of GEN-loaded PLA microsphere (GENMS); (a) pure GEN, (b) PLA microsphere and (c) neat GENMS. (d) and (e) are modified GENMS with 0.35 NaOH and NaOH/ethanol, respectively	138
Figure 4.26	SEM images of modified GENMS. (a) 0.15 NaOH, (b) 0.15 NaOH/ethanol (c) 0.25 NaOH, (d) 0.25 NaOH/ethanol, (e) 0.35 NaOH and (f) 0.35 NaOH/ethanol	140
Figure 4.27	Optical images of drop profiles of neat GENMS and modified GENMS.....	141
Figure 4.28	BSA adsorption on neat GENMS and modified GENMS	144
Figure 4.29	Cumulative GEN release from modified GENMS after 10 days in PBS. (a) 0.15, (b) 0.25 and (c) 0.35 concentration of NaOH and NaOH/ethanol comparing with neat GENMS.....	148

Figure 4.30	XRD patterns of (a) neat CO ₃ Ap scaffolds, (b) GENMS, (c) GEN-CO ₃ Ap scaffold, (d) CS-GEN-CO ₃ Ap scaffold and (e) CS-GENMS-CO ₃ Ap scaffold.....	151
Figure 4.31	FTIR GEN-incorporated into CO ₃ Ap scaffold; (a) neat CO ₃ Ap scaffold, (b), pure chitosan (CS) (c) GEN, (d) GEN-CO ₃ Ap scaffold, (e) CS-GEN-CO ₃ Ap scaffold, (f) GENMS and (g) CS-GENMS-CO ₃ Ap scaffold.....	153
Figure 4.32	SEM images of (a) neat CO ₃ Ap scaffolds (b) GEN-CO ₃ Ap scaffolds, (c) CS-GEN-CO ₃ Ap scaffolds and (d) CS-GENMS-CO ₃ Ap scaffolds. (Images (i) and (ii) were observed at 60× and 2500× magnification, respectively).....	155
Figure 4.33	GENMS in CS layer located at the micropores of CO ₃ Ap scaffolds	156
Figure 4.34	Compressive strength and porosity of scaffolds	157
Figure 4.35	Swelling behaviour of the scaffolds in PBS solution.....	158
Figure 4.36	Cumulative percentage of GEN released in PBS from free GENMS, uncoated and coated scaffolds for (a) 28 days and (b) the enlargement of cumulative GEN release within 24 h	160
Figure 4.37	Mechanism of GEN release from GENMS.....	165
Figure 4.38	Biodegradation of uncoated and coated scaffold for 4 weeks immersion in HBSS at 37 °C	166
Figure 4.39	SEM images of bonelike apatite growth after 3 days immersion on (a) GEN-CO ₃ Ap scaffolds, (b) CS-GEN-CO ₃ Ap scaffolds and (c) CS-GENMS-CO ₃ Ap scaffolds (Left images were observed at 1000× magnification and right images were observed at 7000× magnification)	168
Figure 4.40	SEM images of bonelike apatite growth after 28 days immersion on (a) GEN-CO ₃ Ap, (b) CS-GEN-CO ₃ Ap and (c) CS-GENMS-CO ₃ Ap. (Left images were observed at 1000× magnification and right images were observed at 7000× magnification).....	169

Figure 4.41	Attachment GENMS after 28 days in HBSS	170
Figure 4.42	EDX spectra with Ca/P ratio of (left) GEN-CO ₃ Ap, (middle) CS-GEN-CO ₃ Ap and (right) CS-GENMS-CO ₃ Ap scaffold after 3 days immersion in HBSS	171
Figure 4.43	EDX spectra with Ca/P ratio of (left), GEN-CO ₃ Ap, (middle) CS-GEN-CO ₃ Ap and (right) CS-GENMS-CO ₃ Ap scaffold after 28 days immersion in HBSS	172
Figure 4.44	(Top) Observation of growth inhibition zones against (a, b and c) <i>E. coli</i> and (d, e and f) <i>S. aureus</i> . (Bottom) Quantitative of inhibition zone by scaffolds. Positive and negative control used standard GEN solution and neat CO ₃ Ap scaffold, respectively.....	174
Figure 4.45	Rate of proliferation of hFOB cells grown on control, CS-CO ₃ Ap scaffold, CS-GEN-CO ₃ Ap and CS-GENMS-CO ₃ Ap scaffold for 1, 2, 3, 5 and 7 days incubation.....	176
Figure 4.46	Proposed diagram showing different surface structure by (a) CS-GEN-CO ₃ Ap or GEN-CO ₃ Ap and (b) how the GENMS attach and fill up uneven surface of CS-GENMS-CO ₃ Ap	177

LIST OF SYMBOLS

\AA	Angstrom
a, c	Lattice parameter
cm^{-1}	Reciprocal centimetre
cP	Centipoise
CFU/ml	Colony-forming units per millilitre
k	Constant of Korsmeyer-peppas
K_1	Constant of first-order
K_H	Constant of Higuchi
K_0	Constant of zero-order
kPa	Kilo pascal
M	Molar
mg/ml	Milligram per millilitre
n	Diffusional release exponent
psi	Pounds per square inch
Q_0	Initial amount of drug
Q_t	Amount of drug at time
R^2	Correlation coefficient
T	Time
2θ	Diffraction angle
wt.	Weight
$^{\circ}\text{C}$	Degree Celsius
λ	Wavelength

LIST OF ABBREVIATIONS

ABS	Acrylonitrile butadiene styrene
ACP	Amorphous or nanocrystalline calcium phosphate
ANOVA	One-way analysis of variance
BSA	Bovine serum albumin
CaP	Calcium phosphate
Ca/P	Calcium-to-phosphorous molar ratio
CHN	Carbon, hydrogen, and nitrogen
CO ₃ Ap	Carbonate apatite
DCM	Dichloromethane
DMEM	Dulbecco's modified Eagle's medium
ECM	Extracellular matrix
EDX	Energy dispersive X-ray
ESE	Emulsion solvent evaporation
FTIR	Fourier Transform Infrared Spectroscopy
FWHM	Full width at half maximum
GA	Glutaraldehyde
HA	Hydroxyapatite
HBSS	Hanks' Balanced Salt Solution
hFOB	Human osteoblast cell
ICP-EOS	Inductively coupled plasma optical emission spectroscopy
ICSD	Inorganic Crystal Structure Database
IUPAC	International Union of Pure and Applied Chemistry
MH	Mueller Hinton
MPS	3-(Trimethoxysilyl)propyl methacrylate
PBS	Phosphate buffered solution

PLA	Poly (lactic) acid
PTFE	Polytetrafluoroethylene
PVA	Poly(vinyl) alcohol
rpm	Rotation per minute
SBF	Simulated body fluid
SEM	Scanning electron microscope
TCP	Tricalcium phosphate
XRD	X-ray diffraction

**SFERA MIKRO POLI (ASID LAKTIK) YANG MENGANDUNGI
GENTAMISIN DIGABUNGAN DENGAN KITOSAN MENYALUTI PERANCAH
APATIT KARBONAT**

ABSTRAK

Perkembangan perancah tulang pelbagai fungsi dengan fungsi penghantaran ubat terkawal mempercepatkan pertumbuhan semula tulang. Walaubagaimanapun pengekalan kadar penghantaran ubat dengan pelepasan letusan permulaan yang dikehendaki adalah faktor utama yang mempengaruhi penghantaran antibiotik bersasar untuk mencegah jangkitan pada lokasi kecacatan. Tujuan keseluruhan kajian ini adalah untuk membangunkan perancah karbonat apatit (CO_3Ap) dan digabungkan dengan sfera mikro poli (asid laktik) (PLA) yang mengandungi ubat. Pertama, CO_3Ap dihasilkan dengan mengubah perancah β -TCP melalui rawatan hidroterma. Pengubahan ini dinilai berdasarkan 3 dan 5 kepekatan molar dari larutan Na_2CO_3 dan masa rawatan selama 3, 5 dan 7 hari. Perancah CO_3Ap kemudian disaluti oleh pelbagai kepekatan kitosan (0.5%, 1% dan 2%) untuk meningkatkan kekuatan mampatan. Ejen gandingan silana digunakan untuk meningkatkan lekatan antara permukaan di antara perancah dan lapisan salutan melalui perhubungan kimia. Kedua, sfera mikro PLA yang mengandungi gentamisin dihasilkan melalui kaedah emulsi dan pemeruapan pelarut. Oleh kerana hidrofobik sfera mikro PLA, hidrolisis dengan menggunakan rawatan alkali yang dibantu oleh etanol dikaji untuk meningkatkan kefungsi permukaan PLA. Akhirnya, untuk memasukkan ubat ke dalam perancah, gentamicin sebagai antibiotik untuk aktiviti bakteria spektrum besar telah digunakan. Tiga kaedah memasukkan gentamisin ke dalam perancah telah diselidiki; pemuatan secara terus, disalut dengan kitosan dan disalut dengan sfera mikro yang mengandungi gentamisin

di dalam kitosan. Keputusan yang didapati menunjukkan perancah CO_3Ap mempunyai kandungan karbonat dengan 11 wt.% pada 5 hari rawatan menggunakan 5 molar Na_2CO_3 . Penyalutan perancah dengan bantuan rawatan silana telah meningkatkan kekuatan mampatan 2 kali lebih tinggi daripada tanpa rawatan. Kehadiran kumpulan Si-OH juga telah meningkatkan tumbesaran apatit pada perancah bersalutan bagi ujian bioaktiviti selama 28 hari. Penggunaan etanol dalam rawatan alkali telah meningkatkan hidrofilik mikrosfera PLA dan mengurangkan penyerapan protein sementara mengekalkan kecekapan pengkapsulan ubat yang lebih tinggi. Penghantaran ubat yang terkawal dengan memasukkan sfera mikro PLA yang mengandungi gentamisin ke dalam perancah CO_3Ap telah meningkatkan kadar penghasilan ubat. Ini menunjukkan sfera mikro PLA yang mengandungi gentamisin dalam perancah bersalutan telah memainkan peranan yang bermanfaat dalam melawan jangkitan bagi tempoh masa yang panjang. Perlekatan sfera mikro yang mengandungi gentamicin pada perancah tidak menghalang tumbesaran apatit selama 28 hari ujian bioaktiviti. Malah, lebih kekasaran pada perancah CO_3Ap yang dihasilkan oleh perlekatan sfera mikro PLA meningkatkan lebih banyak penyangkutan kepada sel-sel. Kebolehidupan sel telah ditingkatkan selama 7 hari pengkulturan sel pada perancah tersebut. Dalam kajian ini, keputusan menunjukkan yang sfera mikro yang dimasukkan ke dalam perancah CO_3Ap bersalutan merupakan sistem perancah yang terbaik yang meningkatkan antibiotik dalam penghantaran ubat secara setempat. Sistem ini berpotensi besar bagi menyediakan sokongan mekanikal untuk pertumbuhan semula tisu dengan persamaan komposisi mineral tulang.

GENTAMICIN-LOADED POLY (LACTIC ACID) MICROSPHERE CORPORATED CHITOSAN-COATED CARBONATE APATITE SCAFFOLD

ABSTRACT

The development of multifunctional bone scaffold with the controlled drug delivery functions accelerates bone regeneration. However, sustaining drug release rate with desired initial burst release are main factors that influence a targeted antibiotic release to prevent infection at defect site. The overall aim of this study is to develop carbonate apatite (CO₃Ap) scaffold and incorporated with drug-loaded poly (lactic acid) (PLA) microsphere. Firstly, CO₃Ap was fabricated by transforming β -TCP scaffold via hydrothermal treatment. The transformation was evaluated based on 3 and 5 molar concentrations of Na₂CO₃ solution and treatment time for 3, 5 and 7 days. CO₃Ap scaffold was then coated by various chitosan concentrations (0.5%, 1% and 2%) to improve compressive strength. Silane coupling agent was utilized to enhance the interfacial adhesion between scaffold and coating layer via its chemical link. Secondly, gentamicin-loaded PLA microspheres was fabricated by double emulsion and solvent evaporation method. Due to hydrophobicity of PLA microspheres, hydrolysis by using alkaline treatment which assisted by ethanol was studied to improve PLA surface functionality. Finally, in order to incorporate the drug into fabricated scaffold, gentamicin as antibiotic of broad-spectrum bacteria activity was used. Three methods of loading gentamicin into scaffolds were investigated; direct loading, coated with chitosan and coated with gentamicin-loaded PLA microsphere in chitosan. Results on the CO₃Ap scaffold showed that carbonate content with 11 wt.% was obtained for 5 days treatment using 5 molar Na₂CO₃. Coating scaffold with aided silane treatment improved compressive strength 2 times higher than without treatment.

The presence of Si-OH group also enhanced apatite growth on the coated scaffold for 28 days bioactivity test. Use of ethanol in alkaline treatment improved hydrophilicity of PLA microsphere and reduced protein adsorption while maintained higher drug encapsulation efficiency. A controlled drug delivery by incorporation of gentamicin-loaded PLA microsphere into CO₃Ap scaffold increased drug release rate. This shows gentamicin-loaded PLA microsphere in coated scaffold played beneficial role in combating infection for prolonging time. It is found that adherence of gentamicin-loaded PLA microsphere on scaffold not hindered the apatite growth for 28 days investigation. In fact, more roughness on CO₃Ap scaffold contributed by attachment of PLA microspheres enhanced more anchorage to the cells. Cell viability was improved for 7 days cell culture on that scaffold. In the present study, results showed that, gentamicin-loaded PLA microspheres incorporated in coated CO₃Ap scaffold represents the best scaffold system which improved antibiotic release in a localised drug delivery. The system holds great potential in provide mechanical support for tissue regeneration with similar bone mineral composition.

CHAPTER 1

INTRODUCTION

1.1 Background of study

Every year, millions of people across the world are suffering from bone defects arising from trauma (due to sports, war and road traffic injuries), tumour or bone related diseases. Several are dying due to insufficiency of ideal bone tissue replacement. The current gold standard for bone reconstruction is autologous bone graft but limited availability, donor site morbidity and the need for a second surgery restrict their application (Oryan *et al.*, 2014). The use of allografts as potential alternative to autografts are severely restricted due to the risk of disease transmission and immune response (Romagnoli *et al.*, 2013). Due to these limitations many synthetic materials (biomaterials) are being used as bone substitutes. Therefore, much attention has been diverted to the artificial bone replacement to repair or substitute the fractured bone. These replacements may not damage healthy tissue, do not pose any viral or bacterial risk to patients and can be supplied at any time in any amount (Rodríguez-vázquez *et al.*, 2015).

Ceramics comprise of calcium phosphates (CaPs), silica, alumina, zirconia and titanium dioxide are nowadays used for various medical applications due to their positive interactions with human tissues (Habraken *et al.*, 2007). Among all the ceramics, CaPs are most widely used in the field of orthopaedic and dentistry due to the compositional similarities to human bone (Wopenka and Pasteris, 2005). CaPs have the distinct physiochemical advantages of bioactivity, osteoconductivity, non-toxic and non-inflammatory properties (Dorozhkin, 2018). Hydroxyapatite (HA: $\text{Ca}_{10}(\text{PO}_4)_6(\text{OH})_2$) is one of the most common form of CaP and has been widely used to fabricate porous scaffolds owing to its excellent biological properties including

biocompatibility and osteoconductivity (Li *et al.*, 2017). However, HA is the most stable CaP in the biological environment which having low degradation rate limits its application as bone replacement.

Main mineral component of bone tissue is apatite-like phase which is not pure stoichiometric HA. Various substitutions exist in bone mineral particularly carbonate ions are found up to 8 wt.% with other elements of Na, K, Mg, Zn, Fe, Si and etc that occur at trace (< 1 wt%) levels (Ishikawa, 2010; Nakamura *et al.*, 2016). These elements play an important role in bone physiology. It is well known that the incorporation of carbonate ions has considerable impact on the crystal lattice of apatite structure and on the mineralization process. Introducing carbonate ions in HA increases the resorption rate by osteoclast and could enhance the osteointegration rate compared to HA (Wopenka and Pasteris, 2005). Therefore, carbonate apatite (CO₃Ap) scaffold is a prospective candidate for bone substitute material to mimic the composition of bone tissue and to provide an adequate bone tissue response.

Apart from the composition itself, coating process on CO₃Ap scaffold had also been reported to enhance and stimulate osteoblast cell activity, biodegradability and promote bone remodeling process (Bang *et al.*, 2015). In addition, it is well known that the performance of mechanical properties (e.g. compressive strength, toughness and modulus strength) of fabricated CO₃Ap scaffold would be improved by coating layer (Philippart *et al.*, 2015). Improvement of interfacial adhesion between polymer coating and apatite scaffold can be assisted by chemical link, for example by the silane surface treatment of the scaffold. However, limited studies have been reported on the surface treatment of CO₃Ap scaffold. The silane treatments have been reported to influence the bioactivity, cell adhesion and biocompatibility of scaffold in the presence of active functional groups (Rakmae *et al.*, 2012; Vyas *et al.*, 2017).

Mimicking bone scaffold to natural bone by chemical composition and improved compressive strength is beneficial in tissue engineering. However, the healing process along the scaffold substitution was crucially considered. One of the major problems associated with the use of implants or scaffolds for bone treatment is the occurrence of infections. Effective treatment of defect site is a key challenge in restorative surgery of bone for ensuring successful bone regeneration. Therefore, in enhancing the functionality of the scaffolds, loading therapeutic bioactive molecules such as growth factors or drugs into CaP scaffolds will initiate bone healing in-situ. CaP scaffolds are considered as suitable drug carriers because of their abilities to incorporate and retain the active substance to deliver it locally in a controlled manner over time.

The incorporation of drug-loaded polymer microspheres into CaP scaffold can create multifunctionality of scaffold system. In this study, drug loaded into the polymer-based microspheres was chosen since it shows to an effective controllable release rate in prolonging time compare to the direct incorporating the drug into CaP scaffolds (Sezer *et al.*, 2014). Polylactic acid (PLA) is one of the most frequently used polyesters due to its many favourable properties such as easy availability, biocompatibility and biodegradability.

The capability of fabricated scaffold to bond with living bone is an important factor to determine good osteointegration. This bonding is examined through bonelike apatite formation on their scaffold surfaces. The deposition of apatite on the surface of the scaffolds provide a suitable substrate for cell proliferation resulting in high osteoconductivity as well as osteoinductivity (Vallet-Regí *et al.*, 1999).

Another important point for a biomaterial is evaluation biocompatibility of CO₃Ap scaffold with surrounding bone tissue. The biological performance by cell

activities are fundamental importance in determining good osteointegration. This biological response is influenced by the chemical composition, surface structure and charge and drug delivery factors consisted by bone-substitute materials (Li *et al.*, 2014). In fact, scaffolds with combination of drug-loaded PLA microspheres with greater rough surface may increase cell proliferation. This may guarantee the bone regeneration is successful before the bone grafted totally degrades. Therefore, CO₃Ap scaffold is potentially used as an ideal local drug delivery system for the treatment of implant associated infections. Combination of scaffolds together with healing promoting factors may open new insights in the field of bone tissue engineering.

1.2 Problem Statement

Microbial infection is still one of the most common causes of orthopaedic implantation failure. To address this problem, enhancing functionality of the scaffold as bone replacement and drug delivery agents is a very challenging field for bone tissue regeneration. In developing such scaffold as drug delivery system, various forms of HA have been used in orthopaedic, dental or maxillofacial surgery. HA shows excellent biocompatibility and good osteoconductivity, however, the key drawback of HA is its stability in the bone as foreign substance. In other words, HA is difficult to be resorbed in the bone defect and as a result HA introduces a risk for infection.

The apatite found in human bone is not stoichiometric of Ca₁₀(PO₄)₆(OH)₂ but consisted by other ions mainly carbonate (CO₃²⁻) content and traces of Na⁺, Mg²⁺, Fe²⁺, Cl⁻ and F⁻ (Ishikawa, 2010). Although the presence of these ions is low, they play an important role in the biochemical reactions of bone metabolism. As a result, CO₃²⁻ containing HA has gained much attention due to its chemical composition being closer to bone mineral and favourable for bone growth. High crystallinity and thermal

decomposition of the apatite during the sintering process has restricted the production of CO₃Ap. Because of that, hydrothermal treatment with lower temperature has suitability to fabricate CO₃Ap compared to other methods which require high sintering temperature. Different concentration of carbonate source used, and treatment time may influence the final production of CO₃²⁻ substituted apatite scaffold.

Brittleness of ceramic scaffold can be strengthen using polymer as coating material. Even though the strength will improve, the necessity of biodegradable polymers is also important to be absorbed in host tissue. In fact, factors such as types of polymer and concentration of polymer might influence the scaffold strength. However, the concern in polymer-coated scaffold fabrication is the interfacial adhesion between bioceramics (inorganic phase) and polymer phase (organic phase). The interfacial bond strength within these dissimilar materials totally depends on the mechanical interlock. Due to chemical bonding does not exist in most bioceramics scaffold, surface treatment using silane coupling agents are often used for providing a strong chemical link in coating system. However, limited studies have been conducted to investigate the performance of coated carbonate-substituted apatite scaffold. Most previous researches focused on the silane treatment on composite-based bioceramic (Cisneros-Pineda *et al.*, 2014).

In the last few years, several attempts have been made to investigate the properties of three dimensional of porous scaffolds as a support and as a targeted drug delivery system. The current therapy to prevent implant destructive problem by bone infection relies on systemically administered antibiotics. This conventional treatment poses several major disadvantages. For example, Yazdimamaghani *et al.* (2014) reported that it is difficult to achieve the effective localisation of antibiotics. This therapy is also ineffective once the bacteria anchored and synthesise a biofilm on the

surface of implant. A very high concentration of a drug in bloodstream and other organs easily produce potential side-effects in the body system. Thus, the use of carriers for local antibiotic delivery systems is essential to control drug release in a predictable manner with a specified time.

Drug-containing PLA systems as microsphere have been developed as drug delivery device. However, the main drawback of PLA is high hydrophobicity, which can undergo chain disruption in human body, lack of cell recognition due to non-specific protein adsorption and thus evoke the immune system (Shi *et al.*, 2011). In order to reduce protein adsorption, PLA requires surface treatment to introduce hydrophilic functional groups (Bee *et al.*, 2018). As a carrier in drug delivery system, parameters such as types of treatment method, concentration or types of alkaline solution for hydrolysis treatment and period of treatment time are important to be investigated.

In developing multifunctional scaffold, drug release behaviour of antibiotic-loaded PLA microsphere incorporated in the coated-CO₃Ap scaffold need to be investigated. Due to the hierarchical and complexity of bone structures, comprehensive composition, physical properties and cell interaction in multifunctional scaffold must be critically considered. This is crucial for providing better integration in implantable systems and to guarantee quality of patient's life.

1.3 Objectives

The main objective of this study is to develop drug-loaded PLA microsphere incorporated into chitosan-coated porous CO₃Ap scaffold. The scaffold features must be satisfied to fulfil the requirement for *in vitro* bone tissue engineering to be clinically used as bone grafts. There are some important factors that must be considered

simultaneously for the design and application of this scaffold such as, mechanical strength, porosity, composition and incorporation of therapeutic agent. Therefore, the specific objectives of this work are defined as the following:

- i. To characterize CO₃Ap scaffold produced by gelate-freeze casting method and transformation from β -TCP scaffold using hydrothermal treatment.
- ii. To investigate the effects of silane treatment on the compressive strength, swelling rate, biodegradation, bioactivity and biocompatibility properties of chitosan coating CO₃Ap scaffold.
- iii. To evaluate the effect of alkaline hydrolysis treatment on the surface modification of gentamicin-loaded PLA microsphere.
- iv. To determine the drug release behaviour of chitosan-coated CO₃Ap scaffold incorporated with gentamicin-loaded PLA microsphere
- v. To investigate the biocompatibility and *in vitro* bioactivity of CO₃Ap scaffold in simulated physiological environment using Hank's balanced salt solution (HBSS).

1.4 Scopes of research

This current work was conducted to fabricate a β -TCP scaffold with acceptable pore size, porosity and compressive strength of bone substitution. The β -TCP scaffold was transformed to CO₃Ap scaffold by using hydrothermal treatment in presence of carbonate ions source. The optimized CO₃Ap depending on its crystallinity, carbonate content and cell viability was chosen to be coated with chitosan. Various concentrations of chitosan were used for coating process while silane solution was used to create chemical link between scaffold and coating layer.

In developing a localized drug delivery of bone scaffold, the CO₃Ap scaffold was incorporated with gentamicin-loaded PLA microsphere. In fabrication of gentamicin-loaded PLA microsphere, effect of surface modification using alkaline hydrolysis treatment was studied to examine effects on the encapsulation efficiency and protein absorption properties. CO₃Ap scaffold loaded with gentamicin either loaded in microsphere or directly incorporated in scaffold were investigated. These scaffolds were designed to observe the drug release behaviour for prolonging the release rate at the implantation site. The release kinetic models were also investigated.

1.5 Thesis Organization

This dissertation was organized in the five chapters consecutively. In the first chapter, the introduction of the research work, problem statements, objectives and scopes of the research were explained. In the second chapter, the literature review on several topics including characteristic of bone, development of bone tissue engineering, coating and surface modification on bone scaffold were presented. There also described the incorporation of drug-loaded bone scaffold as a targeted drug delivery system. Lastly, biological performance of bone scaffold reacts in host tissue was explained in this chapter. In the third chapter, materials, procedures of experimental works and characterization techniques performed in this research were described. In the fourth chapter, the results and discussions were comprehensively elaborated. This part discussed the fabrication of β -TCP scaffold and transformation to CO₃Ap scaffold, fabrication of chitosan-coated CO₃Ap scaffold through silane treatment, investigation on effect of surface modification on PLA microsphere using alkaline hydrolysis and development of gentamicin-loaded PLA microsphere

incorporated into CO₃Ap scaffold. In the fifth chapter, the conclusion of the findings and suggestions for the future works were presented.

CHAPTER 2

LITERATURE REVIEW

2.1 Introduction

This chapter consists of seven main sections. The first section focuses on characteristics of natural bone. The second section discusses concern and current materials used in scaffolds fabrication. The third section reviews bone tissue engineering including requirements and fabrication of porous scaffold. The fourth section explains the bone scaffold from ceramics material. The fifth section provides information on the polymers coating on bone scaffold including silane treatment used. The sixth section explains the localisation of bone healing by drug-incorporated scaffolds. The seventh section discusses on the biological performance of bone scaffold and interaction of cell towards the surface properties of biomaterials.

2.2 Characteristic of human bone

In this section, the composition, structure, chemistry, mechanical properties and remodeling of natural bone are reviewed.

2.2.1 Composition and structure of bone

Bone is the basic unit of the human skeletal system. It provides the framework for the body, protects the vital organs, supports mechanical movement, hosts hematopoietic cells and maintains iron homeostasis. Bone has a complex and varying arrangement of structures on broad length scales (Figure 2.1) which enables diverse mechanical, biological and chemical functions. It is important to understand the structural relationship between the various levels of hierarchical structural organization to understand the function of hydroxyapatite (HA) within it. The

macrostructure consists cancellous versus cortical bone while the microstructure consists haversian canal, osteons and lamellae and the nanostructure consists fibrillar collagen and molecular constituents of the tropocollagen, non-collagenous organic proteins, mineral and HA crystal.

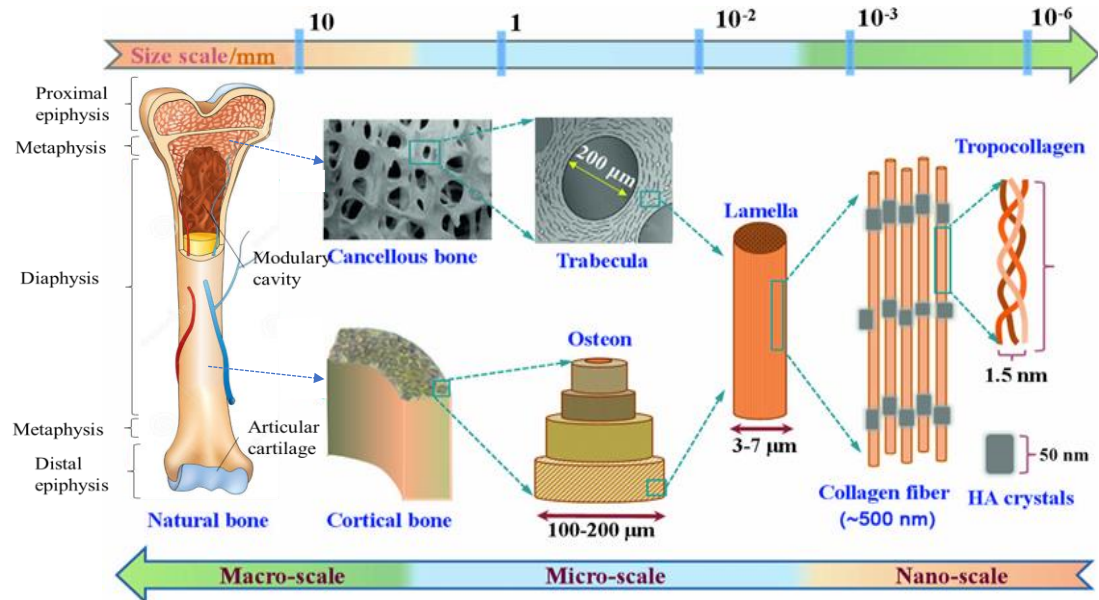


Figure 2.1 The multiscale of natural bone and its composition (Gao *et al.*, 2017)

Bones are usually categorized into two types of cortical (compact) bone and trabecular (spongy or cancellous) bone. In the adult skeleton, the ratio of compact bone and the cancellous bone are 80% and 20%, respectively (Nidhi *et al.*, 2011). Cortical bone forms the outer shell of most bones. It is a dense bone with porosity in the order of 5% to 10%. Trabecular bone usually forms inside of bones that are under compressive stress. Trabecular bone has porosity reaches 50% to 90% (Gao *et al.*, 2017). At the diaphysis, native bone is in close contact with the implant while the metaphysis contains cancellous bone is more reactive that usually provides faster fracture healing (Eliaz and Metoki, 2017).

Besides porosity, the regeneration of specific tissues aided by biomaterials has been shown to be dependent on pore size of the supporting three-dimensional (3D)

structure. Pores are necessary for bone tissue formation because they allow migration and proliferation of osteoblasts and mesenchymal cells, as well as vascularization (Karageorgiou and Kaplan, 2005). Emphasizing from experiments demonstrated that pore size of 100–350 μm is optimum for regeneration of bone (Yang *et al.*, 2001).

Table 2.1 shows the chemical composition of bone. Bone tissue is composed of about 30 % organic matrix, 60 % inorganic mineral matrix and 10 % water by weight (Bellucci *et al.*, 2012). Biological apatites deviate from the stoichiometric composition of HA, $\text{Ca}_{10}(\text{PO}_4)_6(\text{OH})_2$ are usually calcium-deficient (Ca/P molar ratio < 1.67). This is as a results of ion substitution impurities such as Na^+ , Mg^{2+} , K^+ , CO_3^{2-} , Cl^- , F^- , etc in regular HA lattice points (Qin *et al.*, 2007). The quantitative and qualitative content of these impurities vary according to the age and condition of the tissue.

Table 2.1 Chemical composition of bone (wt%) (Eliaz and Metoki, 2017)

Inorganic phase	Organic phase
HA ≈ 60	Collagen ≈ 20
$\text{H}_2\text{O} \approx 9$	Non-collagenous protein ≈ 3
$\text{CO}_3^{2-} \approx 4\text{-}7$	Traces: Polysaccharides, lipids, cytokines
$\text{Na}^+ \approx 0.7$, $\text{Mg}^{2+} \approx 0.5$, $\text{Cl}^- \approx 0.13$	Primary bone cells: osteoblasts, osteocytes,
Traces: Sr^{2+} , Zn^{2+} , Pb^{2+} , Fe^{2+} , Cu^{2+}	osteoclasts

2.2.2 Mechanical properties of bone

Bone is a composite material in which CaP is responsible for the mechanical durability, hardness, rigidity and high resistance to compression while collagen provides elasticity and resistance to tension. Differences in mechanical properties depend on the compartment of bone (corticol versus trabecular bone) as well as the bone orientation. Table 2.2 summarizes the information of the mechanical properties of bone tissues based on the longitudinal direction. The primary function of trabecular bone is to direct stresses to the denser corticol bone (Ruppel *et al.*, 2008).

Table 2.2 Mechanical properties of corticol and trabecular bone (Ramay and Zhang, 2004; Murugan and Ramakrishna, 2005)

Properties	Corticol	Trabecular
Compressive strength (MPa)	100–193	1.9–10
Tensile strength (MPa)	50–150	1.2–20
Strain to failure	1%–3%	5%–7%
Young's Modulus (GPa)	7–30	0.05–0.5

2.2.3 Bone remodeling

Unlike other tissues, bone is a dynamic tissue which can regenerate and repair itself without scar formation. Bone remodeling is a continuous process of bone resorption by osteoclasts and formation throughout lifetime (Karageorgiou and Kaplan, 2005). The bone remodeling units cover around 100 microns of old bone tissue and the average turnover period is estimated at about 3-4 months. It is thought to be regulated by numerous factors including mechanical, vascular, genetic, nervous, nutritional, hormonal and local growth factors (Pivonka *et al.*, 2008).

Three groups of bone cells relate to the bone remodelling are osteoblasts, osteoclasts and osteocytes which have specific roles on bone regulation processes (as shown in Figure 2.2). Osteoblasts secrete bone matrix proteins and they are responsible for formation of new bone tissue. Osteoblasts are also responsible to produce collagen and non-collagenous proteins. Once the osteoblast is finished working it is trapped inside of the bone once it hardens. The trapped osteoblast becomes as an osteocyte. Osteocytes are mature bone cells. Osteoclasts are in charge of absorption of matrix while osteocytes have a function on secreting osseous growth factors promote osteoblastic differentiation and maintaining the matrix (Karageorgiou and Kaplan, 2005). Like osteoblasts, the osteocytes can secrete HA, calcium carbonate and calcium phosphate bone matrix (Kapinas and Delany, 2011). Other osteoblasts remain on the

top of the new bone as lining cells and are used to protect the underlying bone (Karageorgiou and Kaplan, 2005).

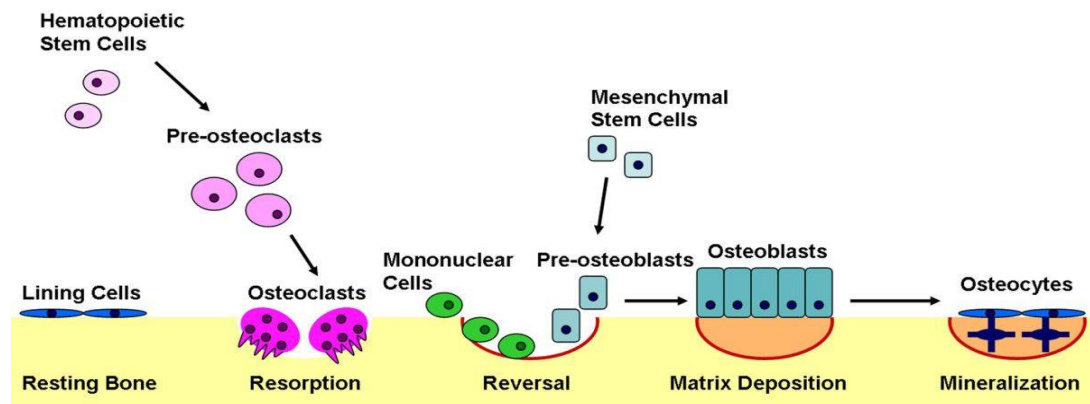


Figure 2.2 Bone remodeling begins with osteoclasts followed by osteoblast and osteocytes (Kapinas and Delany, 2011)

2.3 Concern and current materials used in scaffolds

As reported, several hundred million of individual suffered from musculoskeletal disorders and injuries all around world. The board of the Bone and Joint Decade has emphasized that 50% of the people aged over 65 are affected by chronic joint disease and the number of osteoporotic fractures has doubled in the last 10 years (Nidhi *et al.*, 2011). Bone is the second most commonly transplanted tissue after blood. The annual worldwide market for bone replacement and repair is estimated about \$1 billion, involving autologous, allograft, xenograft and synthetic bone materials. Approximately 90% of these bone graft procedures involve the use of autograft or allograft bone tissue (Al-munajjed *et al.*, 2009).

Autografts are ideal for bone treatment due to their lack of immune rejection. However, this graft possesses some limitations including donor site morbidity, inadequate amount of tissue that can be harvested and inappropriate form. Furthermore, the expenditure of this surgery is expensive and usually patients need receive a long time of medical care after the surgery. Optional treatments by allograft

and xenograft possess its own disadvantages including the possibility of graft rejection by the immune system. In addition, the number of allografts still cannot satisfy the need and supply and potential for disease transmission (Parent *et al.*, 2017).

Even though bone tissue has internal repair and regeneration capacity, healing of large-scale bone defects required grafting to restore function without damaging living tissues. Moreover, due to insufficient blood supply, infection of the bone by the surrounding tissues and systemic diseases can negatively influence bone healing (Yi *et al.*, 2016). Therefore, a huge demand for technologies, materials and bone regeneration strategies to ameliorate such kind of illnesses. Consequently, bone tissue engineering may be a breakthrough technology for the reconstructive treatment of destructive conditions and deformities, since it may provide engineered synthetic bone substitutes with mimicking properties.

Figure 2.3 shows the schematic of the bioceramics evolution used in bone substitution. The development of bioceramics can generally classify into three generations. The first generation is called inert ceramics which aimed to substitute natural bone using zirconia and alumina (Ramakrishna *et al.*, 2001). Although these ceramics are biocompatible, these implants are likely to never transform into bone. The second generation is called bioactive ceramics which aimed to mimic some biomineralization-related functions. Bioactive ceramics yielded promising results in the 1970s. HA and some other CaP composites are typical bioactive ceramics. These bioceramics show excellent biocompatibility properties but medical applications are limited and poor mechanical properties (Haider *et al.*, 2017).

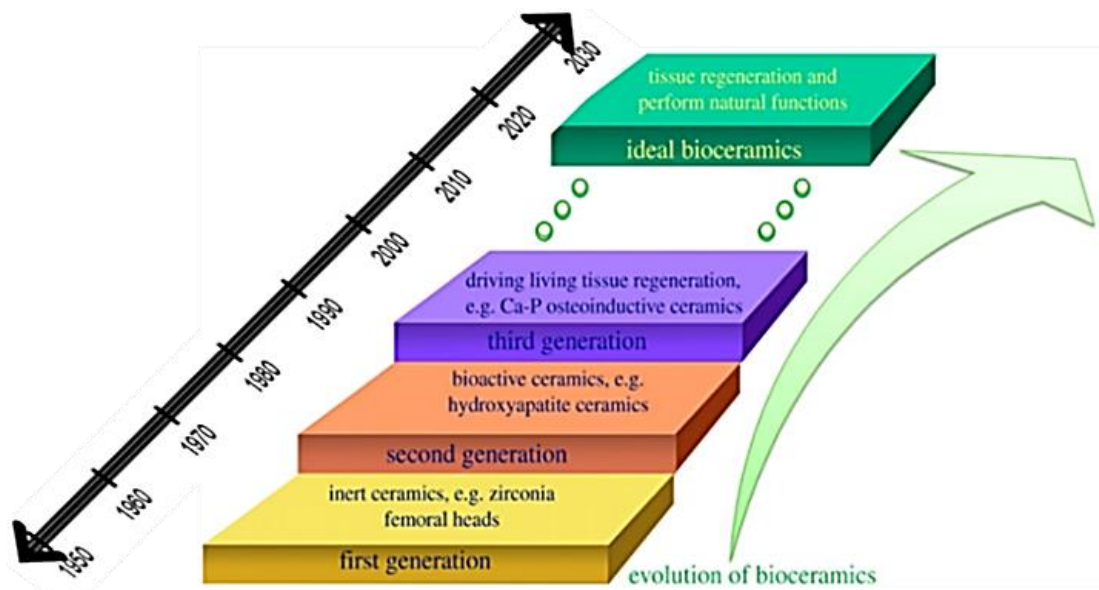


Figure 2.3 A schematic of the evolution of bioceramics (reproduced from Wang *et al.*, 2012)

The third generation of bioceramics is aimed to provide an adequate scaffolding system which can assist the living tissue regeneration (Wang and Yeung, 2017). By optimizing the biomaterials and controlling the implant–tissue interface, the sophisticated implant system can induce tissue regeneration and help to recover it. This generation possess the final purpose of tissue engineering in order to develop artificial materials that can replace and perform the function of biological tissues (Wang *et al.*, 2012; Langer and Vacanti, 1993).

Over the years, the focus of developed biomaterials has addressed biological aspects (Parent *et al.*, 2017). There is an increasing interest to combine bone reconstruction and local drug delivery using CaP scaffolds. However, it demonstrates the wide range of factors that must be considered, and lack of real structure has been approached. This may explain why it is so challenging to design a suitable platform with CaP ceramics loaded with therapeutic substance for bone diseases. According to the database (clinicaltrials.gov), there is currently no clinical trial with such drug

delivery systems. However, cements loaded with antibiotics have been commercially available for years (Wu and Grainger, 2006).

Including growth factors within bioactive scaffolds stimulated cellular growth by allowing inflammatory cells to migrate and trigger the healing process at local injury sites (Romagnoli *et al.*, 2013). In addition, the scaffolds can be incorporated with other types of drug such as antibiotics, analgesics, anticancer, anti-inflammatory. A key issue in these treatments is to maximize the drug access to specific bone sites and be able to control the release of drugs. This is to maintain a desired drug concentration level for long periods of time without reaching a toxic level or dropping below the minimum effective level. Therefore, incorporating a drug-delivery function in bone scaffolds is recognized as highly beneficial in tissue engineering application to facilitate tissue regeneration.

2.4 Bone tissue engineering

In the last decades tissue engineering (TE) has shown tremendous promise in creating biological alternatives for harvested tissues, implants and prostheses. Bone tissue engineering (BTE) is based on the formation of a construct to encourage the regeneration of the damaged tissue. The TE construct is composed of the scaffold, viable cells and signalling (such as biomolecules or bioreactor) as shown in Figure 2.4.

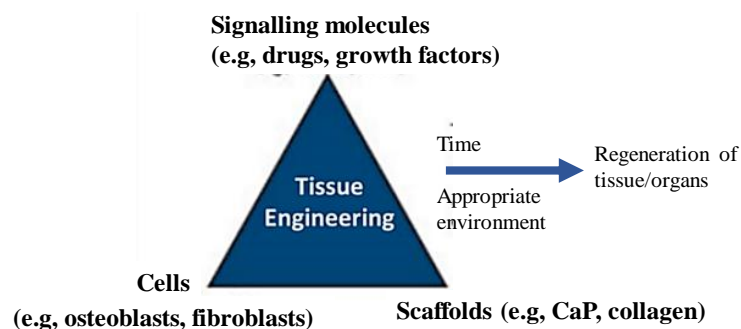


Figure 2.4 Three basic element in TE concept (Swaminathan and Thomas, 2013)

Concept of TE was formally proposed by Langer and Vacanti (1993) who claimed that these synthesized scaffolds have been incorporated with bone marrow stem cells, drugs and gene delivery and different growth factors, such as bone morphogenetic proteins and vascular endothelial growth factor (Wu *et al.*, 2014). Activity of the cells is managed by bioactive molecules incorporated within the scaffold or supplied from the environment. The resulting TE construct is then grafted back into the patient to function as the introduced replacement tissue.

2.4.1 Scaffolds requirements

There are multiple physical and biological requirements that an ideal bone scaffold should address. An optimal bone scaffold replicates the structure and functions of the extracellular matrix (ECM) to provide guidance and support during bone tissue development. Thus, bone scaffold ought to fulfil the accompanying requirements. Interconnected porous is required in promoting vascularisation and facilitate nutrient and oxygen exchange. It may allow the removal of metabolic waste and by-products from cells that have penetrated the scaffolds. The scaffold should match the porosity of cancellous bone at 50–90% and pore sizes of 100–500 μm (Li *et al.*, 2017). These are considered as optimal for encouraging cell attachment, migration and ingrowth throughout the scaffold. In order to match mechanical properties, scaffold should match the compressive strength of cancellous bone with midrange values between 1.9–10 MPa (Murugan and Ramakrishna, 2005).

Besides, an osteoconductive scaffold can be determined by allowing the attachment, growth and ECM formation of bone-related cells into the pores of scaffold to form new bone. An osteoinductive scaffold can differentiate mesenchymal cells into

chondrocytes and osteoblasts and actively induce new bone formation via biomolecular signalling (Dorozhkin, 2018).

Suitable surface roughness is also important to facilitate cell seeding and fixation. The surface energy plays an important role in attracting particular proteins to the bioceramic surface that will affect the cells affinity to the material (Canillas *et al.*, 2017). Scaffolds should have biodegradability at a controlled rate and should keep in the similar speed with bone remodeling rate with no release of toxic or inhibitory products. Thus, it is taking out the requirement for further surgery to remove it (Pande *et al.*, 2016).

The scaffold suitability with the host tissue can be assessed through biocompatibility. This is the most significant factor in the rapid and successful integration of the scaffold. The parameters that reflect the biocompatibility of a material are the absence of cytotoxicity, low or no immunogenicity and absence of carcinogenic effects (Kong *et al.*, 2006). Apart from architecture, scaffolds should be able to deliver bioactive molecules. For example growth factors or drugs can be delivered in a controlled manner to accelerate healing and prevent pathology in order to enhance cell growth (Romagnoli *et al.*, 2013).

Lastly, the scaffold should possess relatively easy processability and be capable of being produced into a sterile product by industrial techniques. Thus, it should be reproducible on a large scale with cost effective processes (Dorozhkin, 2013).

2.4.2 Fabrication of porous scaffold

Depending on the material (polymer, metal, ceramic or composite) to be used, scaffold fabrication techniques differ greatly. The selection of compositions to fabricate the scaffold is very important as this leads directly to the success or failure of a TE strategy. These scaffolds can be developed with the aim of providing not only the physicochemical environment and the structural integrity required for bone regeneration but also with the added value of acting as a local regulator. Hence, the fabricated scaffolds have capability to control the dose and kinetics of therapeutic drug release.

Various of fabrication techniques produced different porous structure and strength of the scaffolds (Darus *et al.*, 2018). However, several of the proposed methods have been conveniently adapted for incorporating growth factors (Mouriño and Boccaccini, 2010) and only a limited number of techniques have been specifically used for fabricating scaffolds with therapeutic drug-delivery capability as summarized in Table 2.3.

Table 2.3 Fabrication methods developed 3D porous bone scaffolds incorporated with therapeutic drug-delivery capability

Fabrication methods	References
Freeze-drying	(Lin <i>et al.</i> , 2015; Fereshteh, <i>et al.</i> , 2016)
Liquid thermally induced separation technique	(Zhang and Zhang, 2002)
Template technique	(Araújo <i>et al.</i> , 2017)
Sol-gel	(Domingues <i>et al.</i> , 2004)
Solvent-casting	(Macha <i>et al.</i> , 2015)

2.5 Bioceramics for bone scaffold

The uses of bioceramics have been revolutionizing the biomedical field for bone repair, regeneration or replacement for the past three decades. They have been

created as either particles, dense blocks or porous scaffolds with uniquely designed shapes and sizes. Bioceramics can be divided into three categories (Yang *et al.*, 2001) namely bioinert groups such as alumina, zirconia, sialon and cermets; bioactive groups such as CaP, bioglass and alumina-wollastonite (A-W) glass ceramic (Asti and Gioglio, 2014) and bioresorbable groups of CaP such as HA, α - or β -tricalcium phosphate, tetracalcium phosphate and octacalcium phosphate.

CaP bioceramics are widely used in the field of bone regeneration, both in orthopedics and in dentistry due to their good biocompatibility, osseointegration and osteoconduction (Eliaz and Metoki, 2017). CaPs are similar to inorganic part of human mineralized tissues (i.e., bone, enamel, and dentin) (Laskus and Kolmas, 2017). CaP has been synthesized and used for fabrication of various forms of porous granules, scaffolds and porous coatings on other implants to improve biocompatibility. Moreover, they may serve as local drug delivery systems to introduce medicines directly into the mineralized tissue (Dubnika *et al.*, 2017). The integration of this biomolecule made the CaP scaffold more osteoinductive (Romagnoli *et al.*, 2013).

There are several types of CaP present as shown in Table 2.4. Different Ca:P molar ratio of each compound would result in different types of CaPs such as di-, tri- and tetra-calcium phosphate, HA and carbonated hydroxyapatite. The Ca/P ratio in CaPs is in the range from 0.5 to 2.0. The stability of CaP in solution generally increases with increasing Ca/P ratios. If CaP has lower solubility than the mineral bone, the CaP will degrade extremely slow and vice versa.

Table 2.4 Chemical composition of CaP (Laskus and Kolmas, 2017)

Compound and chemical formula (correspondent mineral)	Abbreviation	Ca/P ratio
Monocalcium phosphate anhydrous, $\text{Ca}(\text{H}_2\text{PO}_4)_2$	MCPA	0.5
Dicalcium phosphate dihydrate, $\text{CaHPO}_4 \cdot 2\text{H}_2\text{O}$ (monetite)	DCPD	1.0
Octocalcium phosphate, $\text{Ca}_8(\text{PO}_4)_4(\text{HPO}_4)_2 \cdot 5\text{H}_2\text{O}$	OCP	1.33
α and β tricalcium phosphates (TCP), $\text{Ca}_3(\text{PO}_4)_2$ (β -TCP: whitlockite)	α and β -TCP	1.50
Hydroxyapatite, $\text{Ca}_{10}(\text{PO}_4)_6(\text{OH})_2$ (apatite)	HA	1.67
Tetracalcium phosphate, $\text{Ca}_4(\text{PO}_4)_2\text{O}$ (hilgenstockite)	TTCP	2.0
Carbonated hydroxyapatite, $(\text{Ca},\text{Na})_{10}(\text{PO}_4,\text{CO}_3)_6(\text{OH})_2$	CHA/ CO_3Ap	1.7-2.6

The most important requirement for CaP to be bioactive and bond to living tissue is the formation of bone like apatite layer on their surface. In addition, CaP has been reported to support osteoblast adhesion and proliferation (Dorozhkin, 2018). Due to high biocompatibility of CaPs, HA has been widely investigated for its used in various medical applications.

2.5.1 Hydroxyapatite (HA)

Apatite is a structural type for compounds in the general formula of $\text{M}_{10}(\text{PO}_4)_6\text{Y}_2$, being in the case of HA ($\text{Ca}_{10}(\text{PO}_4)_6(\text{OH})_2$). The site of Y and PO_4 is called A site and B site, respectively. The crystal structure of HA is hexagonal (space group $\text{P6}_3/\text{m}$) with lattice parameters, $a = b = 9.432 \text{ \AA}$ and $c = 6.881 \text{ \AA}$. Crystal structure of HA clearly indicates in Figure 2.5.

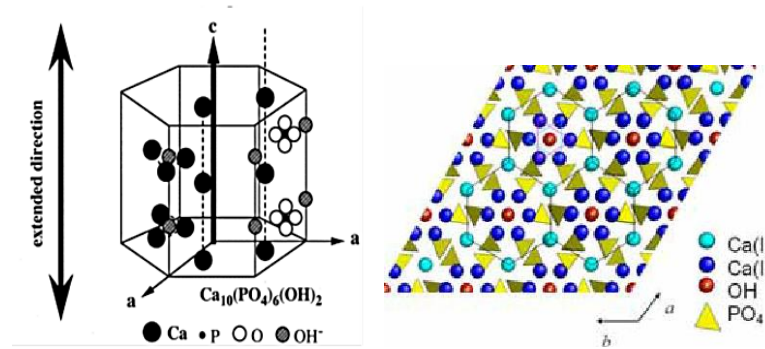


Figure 2.5 Crystal structure of the HA (Wijesinghe, 2014)

For the past 30 years, HA has been popular in orthopaedic, craniofacial surgery, filling bony defects and as a coating on other implants. Among the most interesting property of HA as a biomaterial is its excellent biocompatibility (Parent *et al.*, 2017). HA is considered bioactive, indicating that the ceramic may undergo ionization *in vivo*. The rate of dissolution depends on many factors including, degree of crystallinity (Nagai *et al.*, 2015), crystallite size and porosity (Sheikh *et al.*, 2015). Thus, the synthetic HA is used in hard tissue replacement applications since it is capable of undergoing bonding osteogenesis and is chemically stable for long periods of time *in vivo* (Malafaya and Reis, 2009).

However, the low solubility of sintered HA restricted the application of biodegradation in living tissue. HA scaffolds and particles showed little biodegradation after implantation in long bone segmental defects for 5 years and in the mandible for 9 years (Li *et al.*, 2017). The rate of solubility is 0.1 mg/year in subcutaneous tissue (Park, 2009). Persisting HA at the implantation site interferes with bone formation and is prone to mechanical failure due to its low resistance to crack propagation. Furthermore, due to its low surface reactivity, HA is osteoconductive but not osteoinductive (Erdem, 2012).

As studied by Antoniac (2016), osteoclasts were incubated on the surface of the bone and sintered HA as shown in Figure 2.6. In the case of the bone, resorption

pits were formed on its surface. In contrast, no resorption pits were formed on the surface of sintered HA. It is apparent that sintered HA would not be replaced to new bone since it is not resorbed by osteoclasts and it is not dissolved chemically in the body fluid.

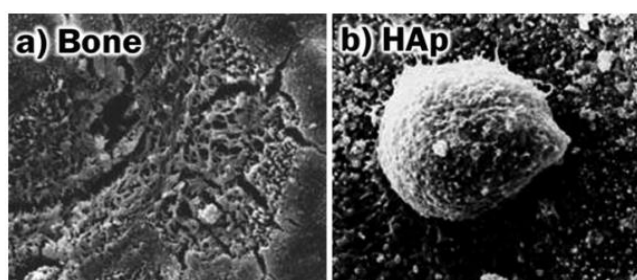


Figure 2.6 SEM image of osteoclasts on the surface of (a) the bone and (b) sintered HA (Antoniac, 2016)

Recent research has attempted to address these drawbacks by making ionic substitutions in the structure of HA (Nakamura *et al.*, 2016). The Ca^{2+} , PO_4^{3-} and OH^- ions can be replaced by other ions, for example fluorapatite and carbonated during processing or in physiological surroundings. Fluorapatite is found in dental enamel while carbonated apatite is present in bone. These substitutions have been shown to improve the bioactivity and biodegradability of HA (Wopenka and Pasteris, 2005).

Production of synthetic HA powders is classified under dry methods and wet methods. The dry route preparation of HA is based on the heat treatment of finely ground mixed precursors. The purity of the final product is dependent upon precise weighing procedures during preparation. Wet methods comprising double decomposition or co-precipitation, emulsion, hydrolysis method, sol-gel method and hydrothermal approach. These methods are widely used due to the simplicity of procedures and allow for perfect control over the structure, texture and morphology (Murugan and Ramakrishna, 2005). Wet methods can be performed in water or in organic solvents by several reactions involving diverse reagents, additives and